

Soliton Propagation in Chains with Simple Nonlocal Defects

R. Burioni¹, D. Cassi¹, P. Sodano², A. Trombettoni², and A. Vezzani¹

¹ *I.N.F.M. and Dipartimento di Fisica, Università di Parma, parco Area delle Scienze 7A Parma, I-43100, Italy*

² *Dipartimento di Fisica and Sezione I.N.F.N., Università di Perugia, Via A. Pascoli Perugia, I-06123, Italy*
(March 30, 2022)

We study the propagation of solitons on complex chains built by inserting finite graphs at two sites of an unbranched chain. We compare numerical findings with the results of an analytical linear approximation scheme describing the interaction of large-fast solitons with non-local topological defects on a chain. We show that the transmission properties of the solitons strongly depend on the structure of the inserted graph, giving a tool to control the soliton propagation through the choice of pertinent graphs to be attached to the chain.

I. INTRODUCTION

Recently, much attention has been devoted to the analysis of complexity arising in discrete physical systems living on networks with non-trivial topologies: remarkable examples are by now given by networks of nonlinear waveguides [1], Bose-Einstein condensates in optical lattices [2], Josephson junction networks (JJN) [3] and silicon-based photonic crystals [4]. In these systems, the choice of the network's topology allows to engineer new macroscopically coherent quantum states: a remarkable example of macroscopic quantum coherence topologically induced by the network topology in JJN has been predicted in [5].

Another relevant area where one should be able to evidence new phenomena induced in discrete quantum systems by the topology is provided by nonlinear dynamical systems. Nonlinearity already produces remarkable phenomena such as soliton propagation [6] even in very simple geometries. A few steps in the study of the interplay between nonlinearity and complex topology have been made: recently, the effects of uniformity break on soliton propagation [7,8] and localized modes [9] have been investigated by considering Y-junctions [7,8] (consisting of a long chain inserted on a site of a chain yielding a star-like geometry) or geometries like junctions of two infinite waveguides or the waveguide coupler [9]. In [10] it has been considered the discrete nonlinear Schrödinger equation (DNLSE) on a discrete network obtained by inserting a finite graph at a site of a one dimensional unbranched chain and the soliton propagation through this finite graph has been studied by numerical and analytical tools. It has been showed that for sufficiently large and fast solitons the soliton momenta for perfect reflection and transmission can be analytically related to the energy levels of the inserted graph. Such results for the transmission properties of solitons in inhomogeneous networks have been used in [11] to show that it is possible to engineer topological filters for the soliton motion on a complex chain.

The simple criterion relating the perfect reflection and transmission momenta and the energy levels of the inserted graph obtained in [10] has been obtained in the situation in which the graph is inserted at a single site.

In the present paper we address the more difficult issue of the soliton propagation for the DNLSE on a network obtained by inserting a graph on *two* sites of an unbranched chain. In this respect, the inserted graph has an internal structure and it is seen by the soliton like an extended topological defect, since during the motion along the unbranched chain the soliton wavefunction is modified in more than one site. One therefore expects a variety of possible resonances between the energies characterizing the soliton propagation and the energy levels of the network. We shall focus here only on some particularly simple inserted graphs: loops, bubbles and single links attached in two sites (see Fig.1). The plan of the paper is the following: after introducing in the next Section the DNLSE on a graph, we report in Section III our results for the transmission properties of solitons on such networks by resorting to numerical simulations and analytical results based on the linear approximation for the analysis of the interaction of fast solitons with these topological defects. Section IV is devoted to our conclusions.

II. THE DNLSE ON A GRAPH

The DNLSE is a paradigmatic example of a nonlinear wave equation extensively studied on regular lattices [12–14]. On a chain it reads

$$i \frac{\partial \psi_n}{\partial t} = -\frac{1}{2}(\psi_{n+1} + \psi_{n-1}) + \Lambda |\psi_n|^2 \psi_n \quad (1)$$

where $n = \dots, -1, 0, 1, \dots$ is an integer index denoting the site position and Λ is the coefficient of the nonlinear term. The normalization condition is $\sum_n |\psi_n|^2 = 1$. It is well known that the DNLSE on a homogeneous chain is not integrable; however, soliton-like wave-packets can propagate with (quasi)momentum k for a long time [15]. By means of a variational approach for gaussian wavepackets with width γ much larger than 1 (the distances are in units of the lattice length), one finds that, for $\Lambda > 0$, it is possible to have solitonic solutions of the variational equations of motion with constant width γ if $\cos k < 0$ and Λ equals the critical value [16]

$$\Lambda_{sol} \approx 2\sqrt{\pi} \frac{|\cos k|}{\gamma}. \quad (2)$$

Numerical simulations confirm that the stability of these wave packet is robust for long times.

The generalization of Eq.(1) on an arbitrary graph is

$$i \frac{\partial \psi_i}{\partial t} = -\frac{1}{2} \sum_j A_{i,j} \psi_j + \Lambda |\psi_i|^2 \psi_i : \quad (3)$$

in Eq.(3) $A_{i,j}$ is the so-called adjacency matrix of the graph [17], which is defined to be 1 if i and j are nearest-neighbours sites, and 0 otherwise. We shall limit ourself to networks obtained inserting simple graphs at two sites of the unbranched chain (Fig.1). The two sites of the unbranched chain at which the graph is inserted are defined to be $n = 0$ and $n = \bar{n}$. We assume that the soliton is traveling from the left with constant velocity v , related to k by $v \simeq \sin k$. Eq.(3) is numerically solved with $\Lambda = \Lambda_{sol}$ using as initial condition

$$\psi_n(t=0) = \mathcal{K} e^{-(n-\xi_0)^2/\gamma^2 + ik(n-\xi_0)} \quad (4)$$

at the sites $n = \dots, -1, 0, 1 \dots$ of the unbranched chain and $\psi_i(t=0) = 0$ at the sites of the added graph. In Eq.(4) \mathcal{K} is a normalization factor and ξ_0 is the initial position of the soliton center: we choose $\xi_0 < 0$ with $|\xi_0| \gg 1$ and $\pi/2 < k < \pi$, so that $v > 0$ and the soliton moves from the left to the right of the unbranched chain. From the numerical solution at very large times (well after the collision with the inserted graph) the reflection and transmission coefficients R and T are computed by the relations $R = \sum_{n < 0} |\psi_n|^2$ and $T = \sum_{n > \bar{n}} |\psi_n|^2$. In the following we shall present numerical results for the coefficients R and T obtained (for an initial width $\gamma = 40$) for different values of k and for the networks plotted in Fig.1.

When the soliton is large ($\gamma \gg 1$) and fast enough that the soliton-defect collision time is much shorter than the soliton dispersion time (i.e. the time scale in which the wavepacket will spread in absence of interaction), thus one may resort to a linear approximation to compute the transmission coefficients [18,19] since, in these limits, the soliton may be considered as a set of non interacting plane waves experiencing scattering on the graph. The soliton transmission coefficients may be then estimated by computing in the linear regime the transmission coefficients of a plane wave across this topological defect inserted at two sites. Afterwards we shall compare our analytical findings with the results coming from the numerical solution of Eq.(3).

III. TRANSMISSION COEFFICIENTS

A. Loops

Let consider the situation in which a loop with length L is inserted at the two neighbouring sites $n = 0$ and

$\bar{n} = 1$ of the unbranched chain [see Figs.1(a,b)]. In the linear approximation, which is expected to be reasonable when $L \lesssim \gamma$, the transmission coefficients may be determined by considering a plane wave solution having

$$\psi_n = a e^{ikn} + b e^{-ikn} \quad (5)$$

for $n \leq 0$, while for $n \geq 1$ one puts

$$\psi_n = c e^{ikn}. \quad (6)$$

At the sites $\alpha = 1, \dots, L$ of the loop the wavefunction is given by

$$\psi_\alpha = d e^{ikn} + f e^{-ikn}. \quad (7)$$

The eigenvalue equation to solve is

$$-\frac{1}{2} \sum_j A_{i,j} \psi_j = \mathcal{E} \psi_i : \quad (8)$$

where i and j run on all the sites of the whole network. Of course, from Eqs.(5)-(6) one obtains $\mathcal{E} = -\cos k$. From the continuity in $n = 0$, $n = 1$, $\alpha = 1$ and $\alpha = L$ one gets, respectively

$$-\frac{1}{2} (a e^{-ik} + b e^{ik} + c e^{ik} + d e^{ik} + f e^{-ik}) = \mathcal{E}(a + b) \quad (9)$$

$$-\frac{1}{2} (a + b + c e^{2ik} + d e^{2ikL} + f e^{-ikL}) = \mathcal{E} c e^{ik} \quad (10)$$

$$a + b = d + e \quad (11)$$

$$c e^{ik} = d e^{ik(L+1)} + f e^{-ik(L+1)} \quad (12)$$

From Eqs.(9)-(12) the reflection coefficient $R = |b/a|^2$ is given by:

$$R = \left| \frac{1 + e^{2ikL} - e^{2ik(L+1)} - 2e^{ik(L+2)}}{1 - 3e^{2ik} + e^{4ik} - 2e^{ik(L+2)} + e^{2ik(L+2)} + 2e^{ik(L+4)}} \right|^2, \quad (13)$$

i.e., $R = R_N/R_D$, where $R_N = 5 - 4 \cos(2k) + 4 \cos(kL) - \cos(2k(L+1)) - 4 \cos(k(L+2))$ and $R_D = 10[1 - \cos(2k) + \cos(kL) - \cos(k(L+2))] + \cos(4k) - 2 \cos(k(L-2)) + \cos(2kL) - 3 \cos(2k(L+1)) + \cos(k(L+2)) + 2 \cos(k(L+4))$. Of course, if one inserts a loop at a single site of the unbranched chain (i.e., $n = \bar{n}$), one has to require $\psi_{\alpha=1} = \psi_{\alpha=L}$ and Eqs.(11)-(12) simply become $a + b = c = d + f$.

The results obtained for the reflection coefficient R from the numerical solution of the DNLS (3) and from the linear approximation, Eq.(13), are reported in Fig.2 for $L = 2$ (circles) and $L = 4$ (crosses) and are in remarkable agreement. We see that for $L = 4$ one has two values of the momenta for which there is perfect reflection ($k \approx 2.10$ and $k \approx 2.25$): this shows that one

can control the soliton propagation by properly choosing the topology of the network. The average position $\langle n \rangle = \sum_n n |\psi_n(t)|^2$ is plotted vs. time in Fig.3. We see that before and after the collision the soliton move with constant velocity: with $v = d\langle n \rangle / dt$, one has $v \simeq \sin(k)$ before the collision, and $v \simeq -\sin(k)$ after the collision which (almost) totally reflects the soliton. The splitting of the soliton in transmitted and reflected parts is illustrated in Figs.4-5, where we consider a loop with length $L = 2$ and $k = 1.8$. In Fig.4 we plot $|\psi_n|^2$ at five different times, including a time ($t = 200$) in which the soliton hits the loop. In Fig.5 we plot the time evolution of the number N_l of particles in the left ($N_l = \sum_{n \leq 0} |\psi_n|^2$), the number N_r of particles in the right ($N_r = \sum_{n \geq 1} |\psi_n|^2$) and the number N_{loop} of particles in the loop ($N_{loop} = \sum_{\alpha=1}^L |\psi_\alpha|^2$): one sees that for $t \approx 200$ the number of particles in the loop increases and after the reflection decreases.

In the simplest case ($L = 1$) a single extra site is attached to the sites $n = 0$ and $\bar{n} = 1$ of the unbranched chain, as in Fig.1(a): then Eq.(13) simplifies to

$$R = \frac{2 \cos^2(k/2)}{2 + \cos k - \cos(3k)}. \quad (14)$$

The comparison between the results for R from the numerical solution of the DNLSE (3) and from Eq.(14) is reported in Fig.6, showing also in this case a good agreement,

We observe that the extra sites of the inserted graph can be view as external Fano degrees of freedom coupled to the chain [19–21]. In particular, in [21] an additional discrete state is coupled to the sites of a straight linear chain: this would correspond in our description to a site linked to all the sites of the unbranched chain.

B. Bubbles

We refer in this Section to inserted p -bubble graphs, i.e. to loops with length $L = 1$ inserted p -times at two sites of the unbranched chains which are distant 2 [see Fig.1(c)]. To fix the notations the sites of the unbranched chain are defined to be $n = \dots, -1, 0_1, 1, \dots$, and other $p - 1$ sites $0_2, 0_3, \dots, 0_p$ are linked to the sites -1 and 1 . Of course, if $p = 1$, we have the simple chain.

The coefficient R may be obtained in the linear approximation in the following way: we assume $\psi_n = a e^{ikn} + b e^{-ikn}$ for $n \leq -1$, $\psi_n = c e^{ikn}$ for $n \geq 1$, and $\psi_0 \equiv \psi_{0_1} = \dots = \psi_{0_p}$ (for symmetry, all the sites inside the bubble are equivalent). The eigenvalue equation (8), with $\mathcal{E} = -\cos k$, in the site -1 reads $-(1/2)(\psi_{-2} + p\psi_0) = \mathcal{E}\psi_{-1}$, i.e.,

$$-\frac{1}{2}(a e^{-2ik} + b e^{2ik} + p\psi_0) = \mathcal{E}(a e^{-ik} + b e^{ik}). \quad (15)$$

Similarly, Eq.(8) in the site $+1$ gives

$$-\frac{1}{2}(p\psi_0 + c e^{2ik}) = \mathcal{E} c e^{-ik}. \quad (16)$$

In a site inside the bubble, Eq.(8) reads

$$-\frac{1}{2}(a e^{-ik} + b e^{ik} + c e^{-ik}) = \mathcal{E}\psi_0. \quad (17)$$

From Eqs.(15)-(17) one gets

$$R = \frac{1}{1 + \left(\frac{p}{p-1}\right)^2 \tan^2 k} : \quad (18)$$

of course, when $p = 1$, no reflection occurs. Eq.(18) shows that increasing k from $\pi/2$ to π (i.e., decreasing the velocity), the reflection increases: slower solitons are more reflected. In this meaning, the p -bubble is an high-pass, i.e. only solitons with high velocity are transmitted: by varying p one can control the width of the range of transmitted velocities. In Fig.7 we plot the reflection coefficient R for $p = 2$ and $p = 20$, showing that a larger p make smaller the range of transmitted velocities. As in Figs.2 and 6, solid lines correspond to the analytical estimate [given by Eq.(18)], and numerical results from the DNLSE (3) are expressed by circles ($p = 2$) and crosses ($p = 20$).

C. Separate links

In this Section we consider the effect on the soliton propagation of two extra sites linked to two sites the unbranched chain, as in Fig.1(d). To fix notations, we suppose that the two extra sites, α and β , are linked respectively to $n = 0$ and $\bar{n} = L$.

To obtain the coefficient R in the linear approximation, one proceeds as before: one assumes $\psi_n = a e^{ikn} + b e^{-ikn}$ for $n \leq 0$, $\psi_n = c e^{ikn}$ for $n \geq L$, and $\psi_n = d e^{ikn} + f e^{-ikn}$ for $n = 1, \dots, L - 1$. The eigenvalue equation (8), with $\mathcal{E} = -\cos k$, in the sites $0, L, \alpha, \beta, 1$ and $L + 1$ reads respectively

$$-\frac{1}{2}(a e^{-ik} + b e^{ik} + \psi_\alpha + d e^{ik} + f e^{-ik}) = \mathcal{E}(a + b) \quad (19)$$

$$-\frac{1}{2}(d e^{ik(L-1)} + f e^{-ik(L-1)} + \psi_\beta + c e^{ik(L+1)}) = \mathcal{E} c e^{ikL} \quad (20)$$

$$-\frac{1}{2}(a + b) = \mathcal{E} \psi_\alpha \quad (21)$$

$$-\frac{1}{2} c e^{ikL} = \mathcal{E} \psi_\beta \quad (22)$$

$$a + b = d + e \quad (23)$$

$$c e^{ikL} = d e^{ikL} + f e^{-ikL}. \quad (24)$$

One has seven unknowns ($a, b, c, d, f, \psi_\alpha$ and ψ_β) and the six equations (19)-(24) (the remaining is provided by the normalization). Solving for b/a one gets

$$R = \left| \frac{1 - e^{2ik} - e^{4ik} + e^{2ikL} + e^{2ik(L+1)} - e^{2ik(L+2)}}{e^{2ik(L+2)} - (e^{2ik} + e^{4ik} - 1)^2} \right|^2. \quad (25)$$

for $L = 1$ Eq.(25) simplifies to

$$R = \frac{(1 + 2 \cos(2k))^2}{9 \cos^2 k + (\sin k + 2 \sin(3k))^2} \quad (26)$$

and for $L = 2$ to

$$R = \frac{(1 - 2 \cos(2k))^2}{4 \sin^2(2k) + (2 \cos(2k) - 1)^2}. \quad (27)$$

Notice that if you have only a site linked to a site of the unbranched chain, one obtains in the linear limit [19,10]

$$R = \frac{1}{1 + 4 \sin^2(2k)} : \quad (28)$$

a comparison of Eq.(28) with Eq.(25) shows the remarkable effect (also for large L) of the second added link on the transmission properties. In Fig.8 we plot the reflection coefficient R for $L = 1$ and $L = 2$, showing that in both situations one has a peak in the transmission ($R \approx 0$) for two different values: the two separate links behave approximately as transmission filters, i.e., allowing for the transmission of solitons with certain velocities. Increasing the distance L between the sites at which the added sites are linked the number of such transmission peaks in turn increases. In Fig.8 the solid lines correspond to the analytical estimate [given by Eqs.(26)-(27)], and numerical results from the DNLS (3) are expressed by circles ($L = 1$) and crosses ($L = 2$).

IV. CONCLUSIONS

In this paper we studied the propagation of large-fast solitons on complex chains built by inserting finite graphs at two sites of an unbranched chain. The inserted graph is seen by the soliton like an extended topological defect: the transmission properties of the solitons strongly depend on the structure of the inserted graph. We considered simple inserted graphs: loops, bubbles and single links. For inserted loops peaks for perfect reflection occurs, while for bubbles the inserted graph behaves as a high-pass filter. When two added sites are linked to two sites having distance L between them, transmission peaks appears and increasing the L the number of such transmission peaks increases. In all these situations we compared numerical findings with the results of an analytical linear approximation, obtaining a good agreement.

In conclusion we think that the study of nonlinear dynamical systems on complex networks is a wide subject to investigate, and that the main motivation of such study is that the network topology provides a natural tool to control the nonlinear dynamics of wavepackets. In particular, we mention as possible interesting future studies the study of the propagation of very localized breathers on complex networks and the nonlinear trapping of solitonic solution in chains with topological defects.

Acknowledgments: We thank P. G. Kevrekidis and B. A. Malomed for stimulating discussions.

-
- [1] Y. S. Kivshar and G. P. Agrawal, *Optical Solitons: from Fibers to Photonic Crystals*, San Diego, Academic Press (2003).
 - [2] M. K. Oberthaler and T. Pfau, J. Phys.: Condens. Matter **15**, R233 (2003).
 - [3] R. Fazio and H. van der Zant, Phys. Rep. **355**, 235 (2001).
 - [4] A. Birner, R. B. Wehrspohn, U. M. Gösele, and K. Busch, Adv. Mater. **13**, 377 (2001).
 - [5] R. Burioni, D. Cassi, I. Meccoli, M. Rasetti, S. Regina, P. Sodano, and A. Vezzani, Europhys. Lett. **52**, 251 (2000).
 - [6] A. C. Scott, *Nonlinear Science: Emergence and dynamics of coherent structures*, Oxford University Press (1999).
 - [7] D. N. Christodoulides and E. D. Eugenieva, Phys. Rev. Lett. **87**, 233901 (2001); Opt. Lett. **26**, 1876 (2001).
 - [8] P. G. Kevrekidis, D. J. Frantzeskakis, G. Theocharis, and I. G. Kevrekidis, Phys. Lett. A **317**, 513 (2003).
 - [9] A. R. McGurn, Phys. Rev. B **61**, 13235 (2000); *ibid.* **65**, 075406 (2002).
 - [10] R. Burioni, D. Cassi, P. Sodano, A. Trombettoni, and A. Vezzani, Chaos **15**, 043501 (2005).
 - [11] R. Burioni, D. Cassi, P. Sodano, A. Trombettoni, and A. Vezzani, Phys. Rev. E **73**, 066624 (2006).
 - [12] D. Hennig and G. P. Tsironis, Phys. Rep. **307**, 333 (1999).
 - [13] P. G. Kevrekidis, K. Ø. Rasmussen, and A. R. Bishop, Int. J. Mod. B **15**, 2833 (2001).
 - [14] M. J. Ablowitz, B. Prinari, and A. D. Trubatch, *Discrete and continuous nonlinear Schrodinger systems*, Cambridge, University Press (2004).
 - [15] B. A. Malomed and M. I. Weinstein. Phys. Lett. A **220**, 91 (1996).
 - [16] A. Trombettoni and A. Smerzi, Phys. Rev. Lett. **86**, 2353 (2001).
 - [17] F. Harary, *Graph Theory*, Addison-Wesley, Reading (1969).
 - [18] X. D. Cao and B. A. Malomed, Phys. Lett. A **206**, 177 (1995).
 - [19] A. E. Miroschnichenko, S. Flach, and B. A. Malomed, Chaos **13**, 874 (2003).
 - [20] S. Flach, A. E. Miroschnichenko, V. Fleurov, and M. V. Fistul, Phys. Rev. Lett. **90**, 084101 (2003).

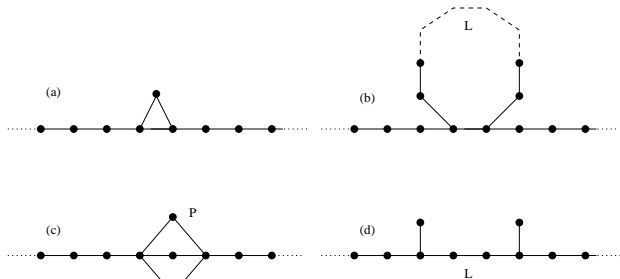


FIG. 1. Inserting simple graphs at two sites of a linear chain: (a) a single extra site attached to two sites of the chain; (b) a loop with length L ; (c) a bubble with $p = 3$ sites; (d) two single links attached at two sites with distance $L = 3$.

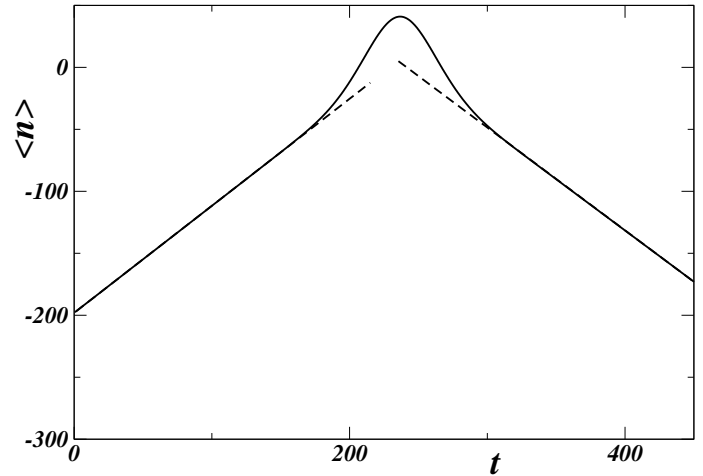


FIG. 3. Center of mass position $\langle n \rangle$ vs. time for $k = 2.1$ and a loop having $L = 4$, which corresponds to perfect reflection. The solid line correspond to the numerical solution of Eq.(3), and the dashed lines to free motion of the soliton with absolute value of the velocity $|v| = \sin k$.

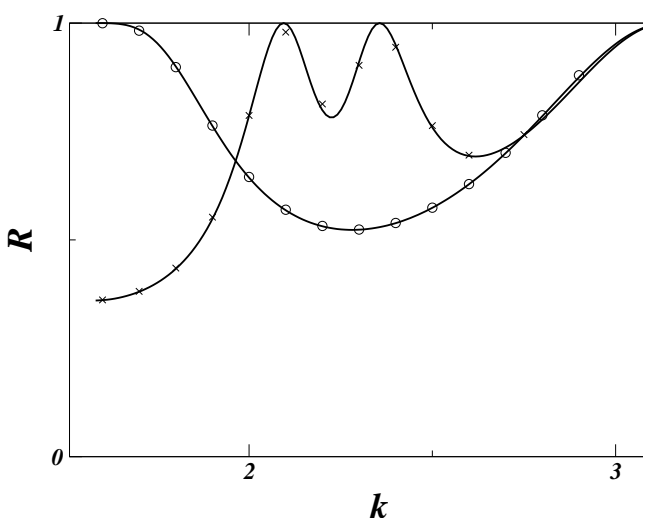


FIG. 2. Reflection coefficient R as a function of k (with k between $\pi/2$ and π) when loops with length 2 and 4 are attached. Empty circles ($L = 2$) and crosses ($L = 4$) correspond to the numerical solution of Eq.(3): as initial condition we choose a Gaussian with initial width $\gamma = 40$ and momentum k (see text). Solid lines correspond to the analytical prediction (13).

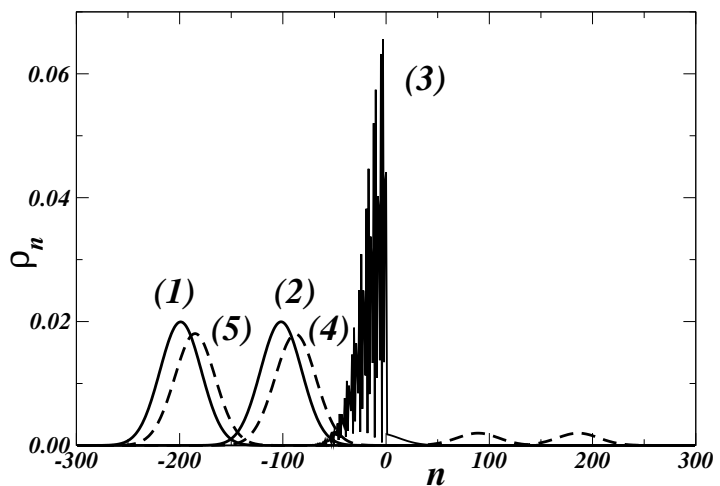


FIG. 4. Soliton propagation obtained from Eq.(3) [for momentum $k=1.8$ and width $\gamma_0 = 40$] through an inserted loop of length 2. The soliton profile is plotted for $z = 0, 100, 200, 300, 400$ corresponding to (1) \dots (5).

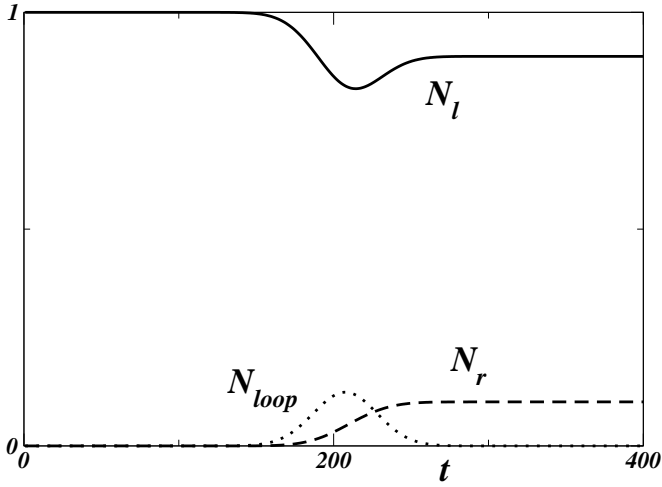


FIG. 5. Time evolution from the numerical solution of Eq.(3) for the number of particles on the left of the loop (N_l), on the right of the loop (N_r) and on the loop (N_{loop}) for $L = 2$ and $k = 1.8$. Around $t = 200$ particles enter the loop (compare with the previous figure).

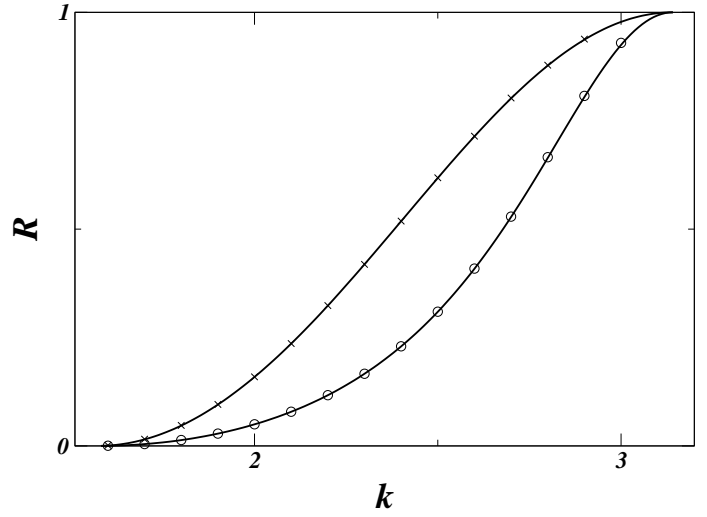


FIG. 7. Reflection coefficient R as a function of k when p -bubbles with $p = 2$ and $p = 20$ are attached. Empty circles ($p = 2$) and crosses ($p = 20$) correspond to the numerical solution of Eq.(3), solid lines correspond to the analytical prediction (18).

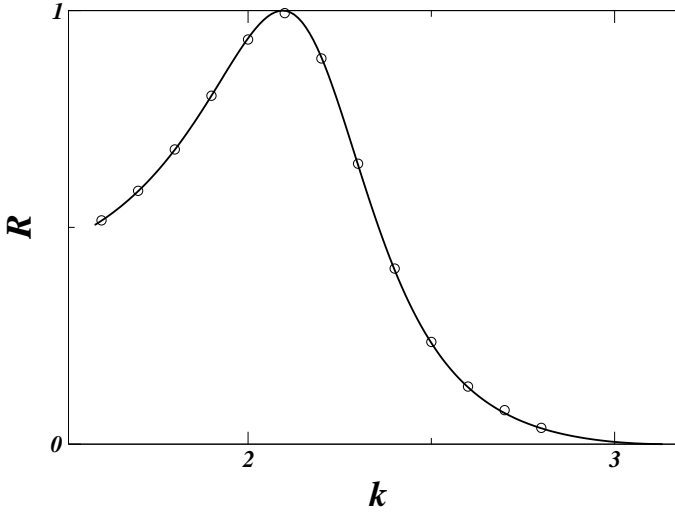


FIG. 6. Reflection coefficient R as a function of k (with k between $\pi/2$ and π) for a loop made of a single site ($L = 1$). Empty circles correspond to the numerical solution of Eq.(3) and the solid lines correspond to the analytical prediction (14).

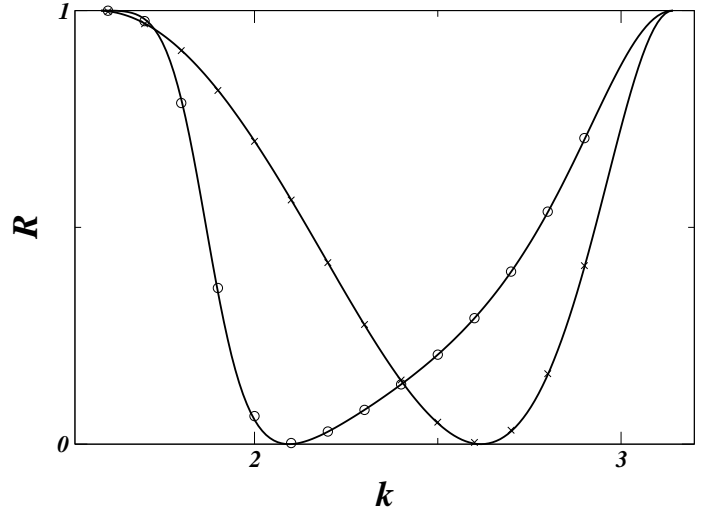


FIG. 8. Reflection coefficient R as a function of k when separate sites are linked to sites distant $L = 1$ and $L = 2$. Empty circles ($L = 1$) and crosses ($L = 2$) correspond to the numerical solution of Eq.(3), solid lines correspond to the analytical predictions (26)-(27).